

# Evaluation of Physical Properties of Volcanic Scoria Powder Particles as Concrete Mineral Additives

Willy Hermann Juimo Tchamdjou<sup>1\*</sup>, Moulay Larbi Abidi<sup>2</sup>, Toufik Cherradi<sup>2</sup>,  
Azzeddine Bouyahyaoui<sup>2</sup> and Didier Fokwa<sup>3</sup>

<sup>1</sup>*Department of Civil Engineering and Architecture, National Advanced School of Engineering, University of Maroua, Maroua, Cameroon*

<sup>2</sup>*Department of Civil Engineering, Mohammed School of Engineers, Mohammed V University of Rabat, Rabat, Morocco*

<sup>3</sup>*Department of Civil Engineering, Higher Technical Teachers' Training College, University of Douala, Douala, Cameroon*

**Keywords:** Volcanic scoria powder, particle size distribution, specific density, surface area and particle morphology.

**Abstract:** This study presents some physical properties relevant to volcanic scoria powder characterization. Specific information on particle shape has been obtained using by 2-D images. The image analysis was used to identify key controls on particle morphology, six shape parameters: elongation, circularity, solidity, roughness, bluntness and luminance have effectively accounted for the morphological variance of powder particles. The particle shape is evaluated according to these six factors. These parameters are scaled to values between 0 and 1.0. Morphological changes associated with variations in the relative size and shape of particles have been quantified. According to results reporting by many authors, it is well known that particle shape analysis, which includes the full range of available grain sizes can contribute not only to the measurements of particle size and shape. But also in providing information on size-dependent densities, specific surface area by Blaine air permeability and specific surface area by laser diffraction.

## 1 INTRODUCTION

Volcanic activities are common phenomena in various parts of the world. Many deposits of volcanic materials are unexploited. Volcanic scoria is a natural volcanic material that is used in many areas such as chemical granular additives, abrasives, dental polisher, cosmetics, pigment, textile, cement, ceramic, and glass industries. In these industries, fine grinding of volcanic scoria granular is generally needed. On the other hand, the development of high-performance cement-based materials like self-compacting concrete and reactive powder concrete has increased the research on inert and semi-inert powders. Today, the characterization of these materials is an emerging subject (Juimo et al, 2017; Tchamdjou et al, 2017a; Tchamdjou et al, 2017b; Bouyahyaoui et al, 2018; Bouglada et al, 2019).

There are many studies focused on the characterization of maximum packing of supplementary cementitious materials (SCMs) in cement-based systems. The related works generally classified the factors that affect the matrix

compactness into four groups: particle morphology, particle packing, interparticle spacing and matrix rheology (Felekoglu, 2009; Arvaniti et al, 2015a; Bouyahyaoui et al, 2018). Particle size and particle shape are closely related to the reactivity of SCMs. Industrial by-products, their partial replacement of cement in concrete mixes represents a substantially offset by the consequent environmental impact. The size and shape characterization of irregular particles is a key issue in many fields of science (Bagheri et al, 2015) and engineering (food, pharmaceuticals, minerals, biology, astronomy,...), which is often associated with large uncertainties (Felekoglu, 2009; Bagheri et al, 2015; Liu et al, 2015; Bouyahyaoui et al, 2018; Dioguardi et al, 2018). The important characteristics of powders are the particle size (granulometry) and particle shape (morphology). Technological properties of powders depend on their granulometry and particle morphology (Pavlović et al, 2010).

To date, only a few studies have been published on particle size and particle shape parameters of mineral powders using as SCMs (Hackley et al, 2004; Felekoglu, 2009; Michel and Courard, 2014; Bagheri

et al, 2015; Klemm and Wiggins, 2017; Bouyahyaoui et al, 2018). Technological properties of mineral powders (bulk density, flowability, surface area, etc.), as well as the potential areas of SCMs, depend on these characteristics (Mikli et al, 2001). It also has been known that powders may improve the particle packing density of cementitious system, and superplasticizers help to obtain the desired rheological properties by increasing the workability without causing segregation in fresh state (Bouglada et al, 2019) and improve the mechanical properties and durability by reducing the water/cement ratio. Some of these powder materials are either industrial by-products or unprocessed materials. They provide environmental relief because industrial by-products are being recycled and hazardous emissions released into the atmosphere due to cement production are reduced, raw materials are preserved and energy is saved (Felekoglu, 2009). Besides, inert and semi-inert powders such as grounded volcanic scoria can be alternatively employed for high-performance mortar and concrete mixture designs (Juimo et al, 2017). More recent works have addressed the effects of volcanic scoria powder addition on rheological properties of cement paste (Tchamdjou et al, 2017a; Tchamdjou et al, 2017b; Bouglada et al, 2019).

Powders are problematic materials in the application of particle size analysis (Felekoglu, 2009). Generally, sizing techniques work best over a limited size range. The optimum range of particle size analysis varies according to many factors, including detector sensitivity and the assumptions associated with the underlying principle of measurement (Felekoglu, 2009; Arvaniti et al, 2015b). Most commercial methods are designed specifically for a range of particle size, and work best with homogeneous spheres. The degree to which irregularity affects the results vary with the technique employed, and is not well understood or exactly accounted for in many methods (Ferraris et al, 2002; Orhan et al, 2004; Hackley et al, 2004; Felekoglu, 2009; Bagheri et al, 2015). The morphology of raw powder includes its particle size distribution (PSD), specific surface area ( $S_{SB}$  or  $S_{SL}$ ) and particle shape. The PSD can be determined by sieves analysis, laser diffraction (LD) and image analysis (IA). The industrial method to determine  $S_{SB}$  is Blaine Air Permeability test (Niesel, 1973; Arvaniti et al, 2015a). The evaluation of particle shape needs complex techniques such as the LD and the IA (Bagheri et al, 2015; Arvaniti et al, 2015b). Individual particle features should be captured by IA to derive the shape descriptors (Ilic et al, 2015; Abazarpour et al, 2017; Bouyahyaoui et al, 2018).

In this paper, in addition to the PSD by the LD, the particle shape and surface morphology of volcanic scoria powders (ground at different grades) were

analyzed by using IA. Some conventional commands of image IAs were employed. Accurate measurements of volcanic powder particle morphology are critical to improving both the understanding of packing processes and the ability to predict particle behavior and the workability of mortar and concrete when using as SCMs.

## 2 EXPERIMENTAL

### 2.1 Powders Samples

Volcanic materials used in this experimental research were supplied from natural deposits of 'Djoungo' (Cameroon). The choice was based on their abundant availability and accessibility. Four volcanic scoria groups according to the colour of scoria (black, dark-red, red, and yellow) have been collected. The collected sample was firstly sieved using the 5 mm stainless steel sieve of 20 cm diameter to separate large volcanic scoria (5–100 mm in order) to fine volcanic scoria ( $\leq 5$  mm). Volcanic scoria aggregates used were between 20 to 50 mm particle size. The volcanic scoria sample was performed on the material dried in an open air environment during 24 h and in the oven at 105 °C during 24 h for the removal of moisture in the rocks (Juimo et al, 2016).

The grinding was performed in a disk mill. Each powder obtained has been described by a two-component code designation: the letter reflecting powder color as black (B), dark-red (DR), Red (R) and yellow (Y) followed by the 'np' reflecting natural powder or natural pozzolan (Juimo et al, 2017).

### 2.2 Measurement Methods

#### 2.2.1 Gas Pycnometer and Blaine Air Permeability (Blaine Fineness, BF)

The density of mineral powders or SCMs is employed in particle size analysis when there is a need to convert from volumetric particle size measurements to mass percentages of particles in a given size range (Arvaniti et al, 2015a). In this work, the density of powders was performed on a Gas Pycnometer. This method measures the density by determining the volume of inert gas that can be introduced into a sample chamber of a defined size which contains a known mass of powder. Automatic Gas Pycnometer has long been identified as the instrument of choice to accurately measure the true density of solid materials by employing Archimedes' principle of fluid displacement, and Boyle's Law of gas

expansion (Niesel, 1973; EN 196-6, 2010). Helium inert gas, rather than a liquid, is used since it will penetrate even the finest pores and eliminate the influence of surface chemistry. This ensures quick results of the highest accuracy. Helium is generally used as the displacement gas due to its size and generally inert behavior. Other gases, such as nitrogen are also routinely used with no measurable sacrifice of performance. The detail data of testing conditions and Gas Pycnometry test results of the measurement processes are present in Table 1. Benefits of the use of Helium Gas Pycnometer are: non-destructive analysis, fast and accurate results (in as little as 1 minute), reliable and reproducible results, a wide range of sample volumes and configurations, the instrument has a small footprint and uses a small amount of gas-pressurized (smaller than 20 Pa, as shown the Table 1).

The fineness of the grinding can be determined according to the Blaine technique and is indicated as the specific surface. The Blaine Air Permeability apparatus serves exclusively for the determination of the specific surface area ( $S_{SB}$ ) of powders. The Blaine fineness (BF) value is not a measure of granulometric distribution (Means PSD). The BF can therefore be used only to a limited degree to evaluate the suitability of a type of test material for a certain use.  $S_{SB}$  or BF value was measured by the Blaine Air Permeability apparatus in this study. The Blaine Air Permeability tester is used for the measurement of the  $S_{SB}$  or BF value of powders as presented by Michel and Courard (Michel and Courard, 2014) based on the air permeability method. The time  $t$  (s) necessary for a volume of air to flow through a packed bed of particles is recorded (Michel and Courard, 2014).

The European Standard EN 196-6 (EN 196-6, 2010) gives the evaluation of  $S_{SB}$  with Kozeny-Carman constant by Equation (1):

$$S_{SB,koz} = K_{app} \frac{\varepsilon^{3/2}}{\rho_s(1-\varepsilon)} \frac{t^{1/2}}{(0.1\eta)^{1/2}} \quad (1)$$

where  $\varepsilon$  is the porosity of the packed bed of powder,  $\eta$  is the viscosity of air (Pa.s) and  $\rho_s$  the density of the solid ( $\text{g/cm}^3$ ). The constant  $K_{app}$  ( $\text{g}^{1/2}.\text{cm}^{3/2}.\text{s}^{-1}$ ), which is a characteristic of the apparatus, is determined with a calibration cement powder linked up to standard reference material. Assuming that the air is compressible (Michel and Courard, 2014), the Kozeny-Carman constant can be used to give a more accurate relationship for the apparatus constant by Equation (2).

$$K_{app} = 10^{-2} \sqrt{\frac{0.1\rho_L D_{cell}}{k C_{air} D_{tube} L_{sample}}} \quad (2)$$

where  $\rho_L$  is the density of the manometer fluid ( $\text{g/cm}^3$ ),  $D_{cell}$  and  $D_{tube}$  are the inner diameters of the

cell and of the tube (cm), respectively,  $k$  is the Kozeny constant,  $L_{sample}$  is the height of the packed bed of powder (cm).  $C_{air}$  is a term which takes into account air compressibility due to pressure drop between the opposite sides of the sample; it depends on atmospheric pressure and geometrical characteristics of the instrument. Kozeny constant ( $k$ ) is related to the shape of particles and the bed tortuosity.

Table 1: Helium gas pycnometer and Blaine air permeability testing conditions, and results.

Test/Parameter	Bnp	DRnp	Rnp	Ynp
Helium Gas Pycnometer (*mean of 04 measurements)				
Weight (g)	1.400	1.698	1.956	1.776
Sample (Vol.)	8.676	8.676	8.676	8.676
Ref. (Vol.)	6.321	6.3215	6.3215	6.3215
Density* ( $\text{g/cm}^3$ )	2.888	3.014	2.920	3.029
Blaine Air Permeability (°mean of 03 measurements)				
T( $^{\circ}\text{C}$ )	21.6	21.6	21.6	22.1
HR (%)	65.5	65.5	65.5	64.5
Weight (g)	2.68	3.35	2.90	2.94
Porosity $\varepsilon$	0.50	0.41	0.47	0.48
$\eta$ ( $\times 10^{-6}$ Pa.s)	18.29	18.29	18.29	18.29
$\rho_L$ ( $\text{g/cm}^3$ )	1.04	1.04	1.04	1.04
$D_{cell}$ (cm)	1.268	1.268	1.268	1.268
$D_{tube}$ (cm)	0.590	0.590	0.590	0.590
$k$ ( $\text{cm.s}^2$ )	340	340	340	340
$L_{sample}$ (cm)	1.478	1.479	1.478	1.480
$C_{air}$ ( $\times 10^3$ Pa)	99.86	99.86	99.86	99.19
$K_{app}$ ( $\text{g}^{1/2}.\text{cm}^{3/2}.\text{s}^{-1}$ )	2.49	2.49	2.49	2.49
Time t (s)	0.74	4.21	0.45	0.05
$S_{SB}$ , Blaine° ( $\text{cm}^2/\text{g}$ )	3596	4482	4674	5227

Equation (2) clearly points out that the apparatus constant depends on several parameters including hygrometric conditions, but also the height of a packed bed of particles: these should be selected in accordance with operational conditions to avoid serious misinterpretation. That's why they propose to calculate Kozeny constant ( $k$ ) linked up to standard reference material and to measure  $L_{sample}$  and  $C_{air}$  for each new test (Niesel, 1973; Michel and Courard, 2014; Arvaniti et al, 2015a).

Table 1 presents also general parameters described below as used during Blaine Air Permeability testing of powders (Bouyahyaoui et al, 2018). The porosity of the packed bed  $\varepsilon$  of powder during the Blaine Air Permeability testing ranges between 0.41 - 0.50 (41 to 50 %) as reported in Table 1. Juimo et al. (Juimo et al, 2016) are reported that VSA size between 20-50 mm can present up to 51% of porosity. These results show that the porosity of volcanic powder is also higher like the porosity of volcanic scoria aggregates (Juimo et al, 2016). According to that fact, the porosity of volcanic scoria can be supposed to be a higher-scale porosity (Bouyahyaoui et al, 2018).

### 2.2.2 Laser Diffraction (LD)

The granulometry of powders can be determined by many methods (sieve analysis, LD, IA, etc.), but the question is how adequately they describe the powder granulometry (Mikli et al, 2001). Mikli et al. (Mikli et al, 2001) reported that the evaluation of the fine powder granulometry (with particle size less than 50  $\mu\text{m}$ ) is more difficult and the results of the sieve analysis do not describe adequately the powder granulometry. For this reason, the first method used here to describe powder granulometry is LD. LD which is based on a complex theory of interaction between monochromatic light and individual particles. This involves the detection of the angular distribution of light scattered by a set of monodispersed spherical particles to provide a 'sphere'-equivalent size diameter distribution using a reverse optical scattering-based model calculation (Michel and Courard, 2014).

In LD, the angular distribution of light is measured after passing through an optically dilute dispersion of suspended particles. The LD system determines the PSD based on a volumetric basis. The volumes of particles are calculated using the density of scattered laser light. This technique is widely used in dust and mineral industry, with water and dispersive agent to a special cell where the laser light is sent (Felekoglu, 2009; Orhan et al, 2004). Different optical models are commonly used to build the PSD weighted by apparent volume (volume of an equivalent sphere of diameter  $D$ ), such as Mie theory-based and Fraunhofer models (Michel and Courard, 2014; Varga et al, 2018).

Fraunhofer approximation is a simplified approach and the knowledge of refractive index and absorption coefficient is not required, since it is assumed that the measured particles are relatively large (over 25-30  $\mu\text{m}$  - about 40 times larger than the wavelength of the laser light) and opaque (Varga et

al, 2018). Fraunhofer approximation model was used during the wet dispersion measurement processes. Wet dispersion measurements were performed using a Mastersizer 2000 instrument coupled to a Hydro 2000S wet dispersion unit. Volcanic scoria powders were dispersed in a sodium pyrophosphate solution. Then, the samples were transferred to a dispersion unit that contained deionized water. LD was repeated three times on each powder sample.

General measurement conditions by Mastersizer 2000 instrument of powders are given in Table 2. The concentration of particles in deionized water ranged between 0.0082 to 0.0112, with a particle refraction index and absorption equal to 0. The refraction index of deionized water was 1.33.

Table 2: General measurement conditions for the laser diffraction (LD) of each powder.

Sample Name	Bnp	DRnp	Rnp	Ynp
Concentration (%)	0.0112	0.0088	0.0104	0.0082
Dispersant RI	1.33	1.33	1.33	1.33
Stirrer speed	2,870	2,870	2,870	2,870
Ultrasonic level	50	50	50	50
Residual – weighted (%)	1.019	0.874	0.880	1.073
Obscuration* (%)	15.40	17.02	18.03	14.76
Pump speed	2,870	2,870	2,870	2,870
RI : Refractive Index ; *Percentage of incident light that is attenuated due to extinction (scattering and/or absorption) by the particles				

An estimation of another specific surface area ( $S_{SL}$ ) is calculated using data from the PSD by LD measurement, following the Equation (3).

$$K_{app}S_{SL} = \frac{6}{\rho_s \cdot D[3,2]} \quad (3)$$

where the volume to surface mean diameter  $D[3,2]$  of the sample is calculated from the size distribution curve by means of Equation (4), and volume mean diameter  $D[4,3]$  in which  $n_i$  corresponds to the number of particles of diameter  $d_i$ . These equations assume that the particles are spherical and that they are not porous.

$$D[3,2] = \frac{\sum n_i d_i^3}{\sum n_i d_i^2} \text{ and } D[4,3] = \frac{\sum n_i d_i^4}{\sum n_i d_i^3} \quad (4)$$

The  $S_{SB}$  obtained by Blaine Air Permeability was compared by  $S_{SL}$  obtained based on data from PSD by LD.

### 2.2.3 Image Analysis (IA)

IA has made a decisive breakthrough in the recent years to become a reference technique in the field of combined size and shape analysis of particles (Gregoire et al, 2007; Arvaniti et al, 2015b; Jia and Garboczi, 2016). The IA is a method for the measurement of particle size and shape distributions. For the measurement of particle size and morphometric characterization, an Occhio 500 Nano image analyzer has been used.

The Occhio 500 Nano image analyzer is an optical analyzer for the characterization of the particle morphology on a two-dimensional projection area ( $A$ ). The instrument includes an integrated vacuum dispersion system and a high-quality optical component which allows assessing size and shape of a set of dispersed particles. Few milligrams of particles are dispersed on to a circular glass slide which is moved in front of a collimated violet backlighting (Michel and Courard. 2014).

Pictures of individual particles capture with a higher resolution camera fitted with a telecentric lens (Arvaniti et al, 2015b). A full description of the instrument and all relevant features can be found at Occhio's website (<http://www.occhio-usa.com>). After performing automated static IA by Occhio 500 Nano image analyzer, it is possible to identify key controls on particle morphology using size and shape parameters obtained. Size parameters (inner diameter, area diameter, width, length, max distance, geodesic length) describe a geometrical object independently of its shape. Size factor descriptors, illustration and definition generally employed are presented in Table 3.

The morphology of a powder particle is characterized by shape description (elongation, circularity, solidity, roughness, bluntness (with the calypter), luminance) or quasi-quantitatively, for example, by means of geometrical shape parameters. Shape factor descriptors, illustration and definition generally employed are presented by Table 4.

Table 3: Size factor descriptors, illustration and definition generally employed.










Size descriptor	Symbol	Definition	Illustration
Number of particles the of powder sample	$N_p$	The number of particles contained in the testing sample.	
Projection area	$A$	The perimeter of the convex hull ( $P_C$ ) is the perimeter length of the convex hull (envelope) that bounding the particle.	
Area of the convex hull	$A_C$	The area of the convex hull ( $A_C$ ) is the area of the smallest convex hull that contains the projection of the particle.	
Perimeter of the convex hull	$P_C$	The perimeter length of the convex hull (envelope) that bounding the particle.	
Inner Diameter	$X_{DI}$	The inner diameter ( $X_{DI}$ ) is the diameter of the maximum inscribed circle (the maximum circle lying completely inside the particle) or the biggest circle inscribed into the projection area of the Particle.	
Area Diameter	$X_{DA}$	The area diameter ( $X_{DA}$ ) is the diameter of a circle having the same area as the particle.	
Width and Length	$W_b$ $L_b$	The width ( $W_b$ ) and the length ( $L_b$ ) are defined as the projection of the particle on the inertia ellipse minor and major axes, respectively. These are Feret diameters in the direction of the inertial ellipse axes. Aspect Ratio ( $A_R$ ) is defined as ratio of width by length. $A_R = \frac{W_b}{L_b}$	
Max Distance	$X_{DM}$	The max distance ( $X_{DM}$ ) is the maximum distance found within the particle.	
Geodesic length	$X_{LG}$	The geodesic length ( $X_{LG}$ ) is a better approximation of the particle length and width of a very long and concave particle (fiber).	

Table 4: Shape factor descriptors, expression and definition generally employed.

Shape descriptor	Definition / Expression
Elongation ( $E_l$ )	Elongation ( $E_l$ ) is defined as the ratio between the width and the length of the particle. $E_l = 1 - \frac{W_b}{L_b}$
Circularity ( $C_c$ )	Circularity ( $C_c$ ) is the degree to which the projection area of the particle is similar to a circle, considering the smoothness of the perimeter. Values are in the range [0, 1]. $C_c = \sqrt{\frac{4\pi A}{P^2}}$
Solidity ( $S_d$ )	Solidity ( $S_d$ ) is a measure of the overall concavity of the projected area of the particle. Solidity is the object area divided by the area enclosed by the convex hull. Values are in the range [0, 1]. $S_d = \frac{A}{A_c}$
Roundness ( $R_d$ )	Roundness ( $R_d$ ) is a useful parameter for describing the similarity degree of a particle to a circle. Values are in the range [0, 1]. $R_d = \frac{4A}{\pi X_{Fmax}^2}$
Roughness ( $R_g$ ) (Occhio Roughness)	Roughness ( $R_g$ ) is the ratio of smooth reference to the particle projection area. This is the Roughness index. Roughness is the amount of material to be removed from the shape before getting a smooth surface. Values are in the range [0, 1]. $R_g$
Bluntness ( $B_t$ ) (Occhio Bluntness)	Bluntness Index ( $B_t$ ) is the expression of a “maturity in the abrasion process”. It is based on a very accurate measure of local curvature and takes into account the fact that very acute asperities wear off almost instantaneously as compared to blunt ones. This had been observed for a long time by geologists working on natural stream sediments. From their observations and definitions, visual charts (Krumbein/Sloss) had been defined and largely diffused among scientists and engineers. Values are in the range [0, 1]. $B_t = \frac{1}{\sqrt{\bar{V}-1}}$ , which: $\bar{V} = \frac{1}{N} \sum_i^N \left(1 + \frac{r_{max}}{r_i}\right)^2$
Luminance ( $L_m$ )	Luminance ( $L_m$ ) is the mean value of the luminance of pixel inside the projection area of the particle. The luminance is the mean greyscale level of the particle. Value ‘0’ corresponds to a black particle, when the value increases the particle is more and more clear. Values are in the range [0, 1].

The shape parameter characterizes mainly the shape, without considering the size (Mikli et al, 2001; Jia and Garboczi, 2016). The description of each parameter in Table 3 and Table 4 is based on Occhio 500 Nano image analyzer manufacturer (www.occhio.be).

The question of representativity of analysis samples by the IA has not been discussed in statistical terms. The IA is based on the measurement of each particle; the accuracy of a size and shape distribution has to be formulated in number of particles ( $N_p$ ) and not in terms of sample weight or duration of the analysis.

The adequate particle number is linked to the shape of the distribution curve and its extension or range (Gregoire et al, 2007). Volcanic scoria powders tested by the IA had respectively: 24,268 particles for Bnp, 32,302 particles for DRnp, 22,562 particles for Rnp and 25,041 particles for Ynp. Morphology of powder particles was performed by the IA by 2D projection.

The bulk results data of these IA tests have been reported firstly by Bouyahyaoui et al. (Bouyahyaoui et al, 2018). In this work, their statistical analysis were performed with the view to providing some correlations between several physical properties of particles from volcanic scoria powders for more understandings.

## 3 RESULTS AND DISCUSSION

### 3.1 Principal Properties

The principal characteristics mean of VS powders performed by Helium Gas Pycnometer, Blaine Air Permeability, LD and static IA are reported in Table 5. The powders obtained have a density between 2.8 and 3.1 g/cm<sup>3</sup> and SSA Blaine between 3,500 and 5,300 cm<sup>2</sup>/g, which are comparable to OPC fineness (Bouyahyaoui et al, 2018; Juimo et al, 2017).

By LD, mean particle diameter (Dmed), mean particle diameter of 10% of particles D(10), median particle diameter D(50) and mean particle diameter of 90% of particles D(90) were measured to evaluate the efficiency of the milling process. Using the PSD data obtain by LD and Equations (3)-(4),  $S_{SL}$  evaluated are ranging between 4,400 to 6,000 cm<sup>2</sup>/g.

PSDs of powders were evaluated by using the LD and IA. The PSDs of powders were plotted in Figure 1a and Figure 1b, respectively, and PSD main significative measurement parameters are presented by Figure 1c. In the LD technique, the angular distribution of light is measured after passing through an optically dilute dispersion of suspended particles. This technique is widely used in dust and mineral industry with water and dispersive agent to a special

cell where the laser light is sent (Felekoglu, 2009; Orhan et al, 2004).

The inscribed disk diameter ( $X_{DI}$  or  $X_{DA}$ ) of each particle is calculated in real time to build PSD curves weighted by apparent volume (Gregoire et al, 2007), making the assumption that particles have identical flatness ratios, whatever their size (Michel and Courard, 2014). Area diameter of particles was used to plot PSD curve obtained by IA (cumulative volume and by volume). The PSD profile shows a negligible difference in the results by the two methods (Abazarpour et al, 2017). The main reasons for differences between two PSD methods are as follows: the considerate particle diameter by each measurement process, the different shapes of the particles; better insight into particles using the IA method; insufficient dispersion of fine particles; fine particles adhering to the bigger particles (Figure 1). LD and 2D projection image by the IA are commonly used the PSD measurement techniques, but the results may not be representative of the strongly true

physical dimensions of the particles (Califice et al, 2013).

Table 5: Helium Particle Size Distribution Characteristics of Powders by LD and IA.

Physical properties	Bnp	DRnp	Rnp	Ynp
Granulometry by Laser Diffraction (LD)				
Dmed ( $\mu\text{m}$ )	48.639	22.401	37.971	27.777
D[3,2] ( $\mu\text{m}$ )	4.706	3.318	3.674	3.621
$S_{SL}$ , LD ( $\text{cm}^2/\text{g}$ )	4,414	5,999	5,593	5,470
Granulometry by images analysis (IA) (D: Area Diameter)				
D <sub>MEAN</sub> ( $\mu\text{m}$ )	46.99	70.55	39.22	33.56
D <sub>MIN</sub> ( $\mu\text{m}$ )	0.593	0.593	0.593	0.593
D <sub>MAX</sub> ( $\mu\text{m}$ )	105.3	150.4	72.08	79.33

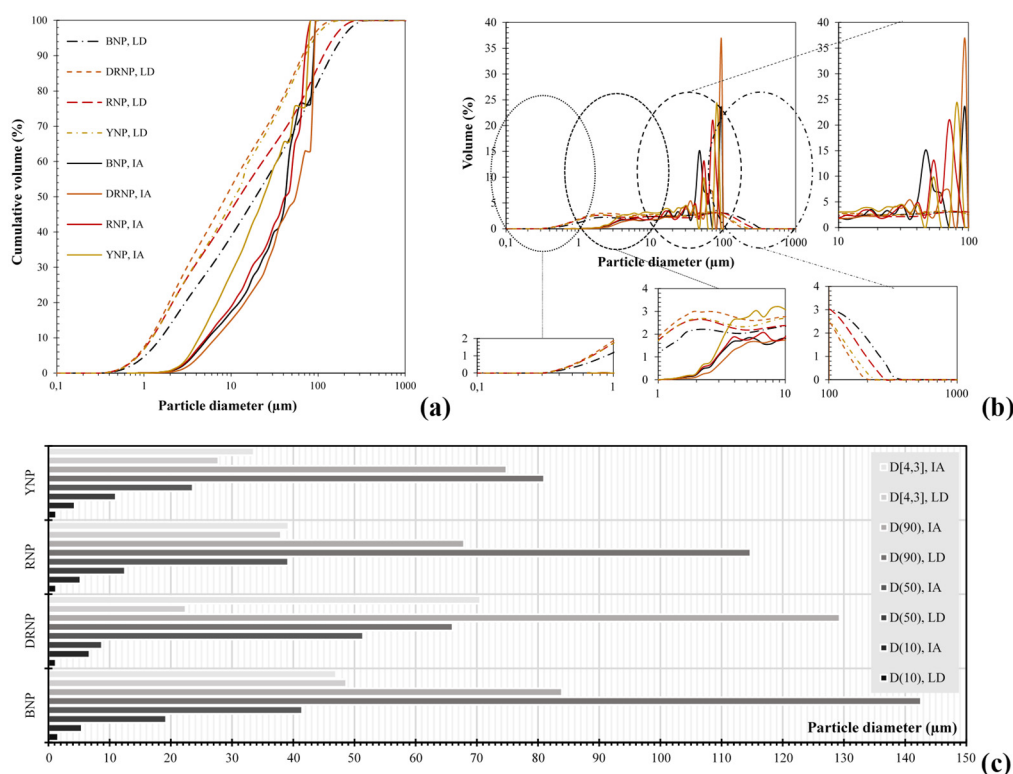


Figure 1: Theoretical PSD results by LD and IA: (a) cumulative volume curve, (b) volume curve and (c) principal PSD descriptors.

### 3.2 Particle Morphology Analysis

More than 50 images of powder particles were identified. The main principal particles identified for

each powder are presented by Figure 2 (17 particles from Bnp, 10 particles from DRnp, 12 particles from Rnp and 11 particles from Ynp).

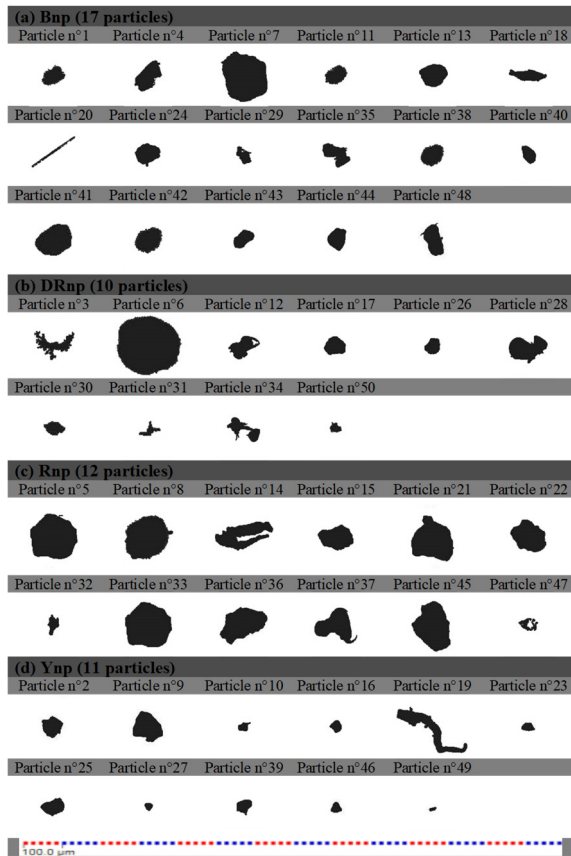


Figure 2: Some particles clearly identified and selected for evaluation from the original images of powders (a) Bnp, (b) Drnp, (c) Rnp and (d) Ynp.

The particle morphology was found to provide reasonable accuracy for estimating the particle sizes

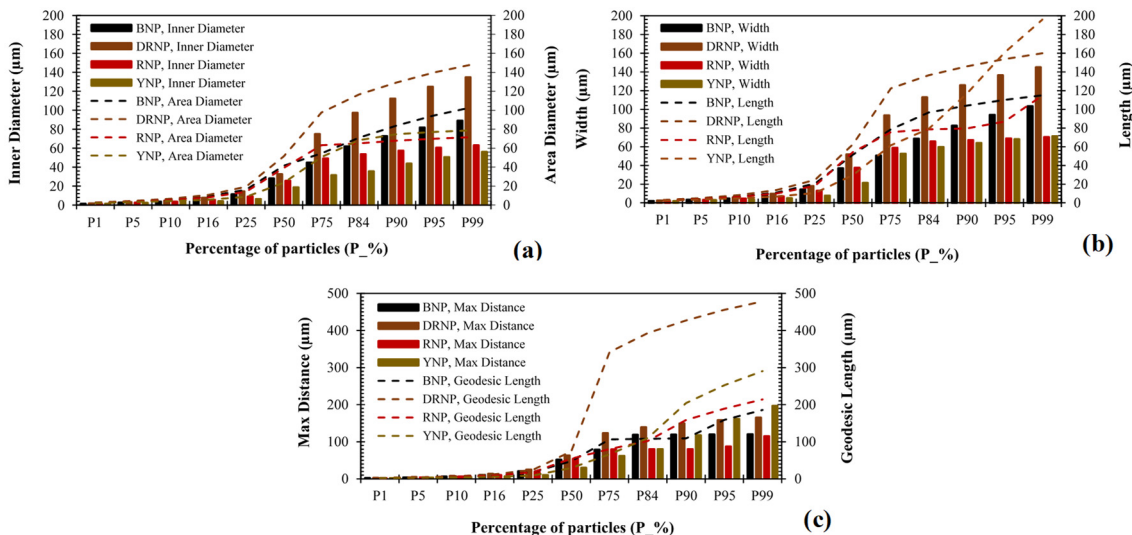


Figure 3: Distribution of (a) inner diameter and area diameter, (b) width and length, and (c) max distance and geodesic length of particles of each powder.

of highly porous particles (i.e. particles n°3, n°10, n°12, n°14, n°47,...), where the distinction between inter-particle and intra-particle porosity was made.

This important comment concerning inter-particle and intra-particle porosity has been also reported by Klemm and Wiggins (Klemm and Wiggins, 2017).

PSDs can be displayed by apparent volume and a number or range of particles. Figure 3a shows the distribution of inner diameter and area diameter of particles of each powder. About 10% of the first very fine particles of these powders have about the same inner diameter and area diameter means. The area diameter is always higher than the inner diameter (Tierrie et al, 2016). The results show the inner diameter used in the IA systems can perfectly represent the sieve size of a particle (He et al, 2016).

Figure 3b shows the distribution of width and length of particles of each powder. About 10% of the first very fine particles of these powders have about the same width and length means. The length is always higher than the width.

Figure 3c shows the distribution of max distance and geodesic length of particles of each powder. About 5% of the first very fine particles of these powders have about the same max distance mean and geodesic length mean. The geodesic length is generally always higher than the max distance.

Figure 4a shows the distribution of elongation and circularity of particles of each powder. The circularity is always higher than the elongation. The particle elongation appears to be quite low with 75 % of the particles getting an elongation ratio lower than 0.40.



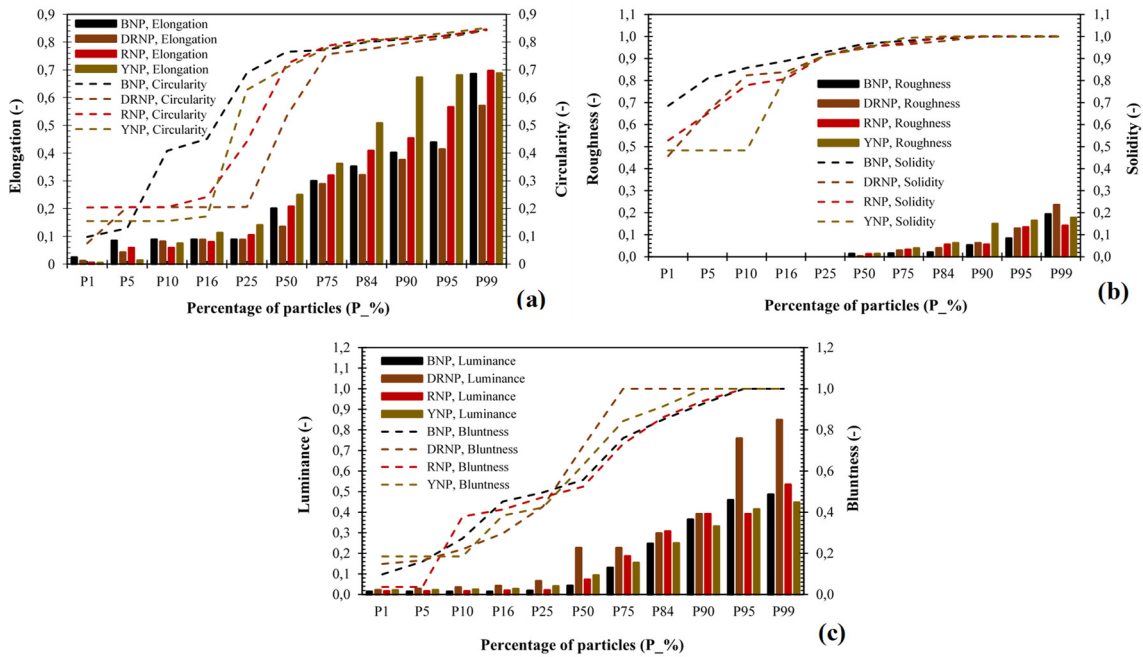


Figure 4: Distribution of (a) elongation and circularity, (b) roughness and solidity, and (c) luminance and bluntness of particles of each powder.

On the contrary, the particle circularity appears to be high with 75% of the particles getting circularity ratio higher than 0.40.

Figure 4b shows the distribution of roughness and solidity of particles of each powder. The solidity ratio is always higher than the roughness ratio. With all particles getting a roughness ratio lower than 0.25 and a solidity ratio higher than 0.45.

Figure 4c shows the distribution of luminance and bluntness of particles of each powder. The bluntness ratio is always higher than the luminance ratio. The particle bluntness appears to be high with 75% of the particles getting a bluntness ratio higher than 0.40. On the contrary, the particle luminance appears to be low with 90% of the particles getting a luminance ratio lower than 0.40. Figure 5 shows the general classification according to shape parameters considered, of 50 particles identified from IA set data. The shape parameters are scaled to values between 0 and 1.0. Consider all powders, the higher value of elongation, circularity, solidity, roughness, bluntness and luminance are 0.822, 0.843, 0.967, 0.165, 1.000 and 0.759 respectively (Figure 5). The higher value to express roughness of these particles is non-significant (0.165) and indicates that these particles have globally a bad roughness. In another part, the ultra-low value of elongation, circularity, solidity, roughness, bluntness and luminance are 0.088, 0.129, 0.483, 0.013, 0.160 and 0.066 respectively (Figure 5).

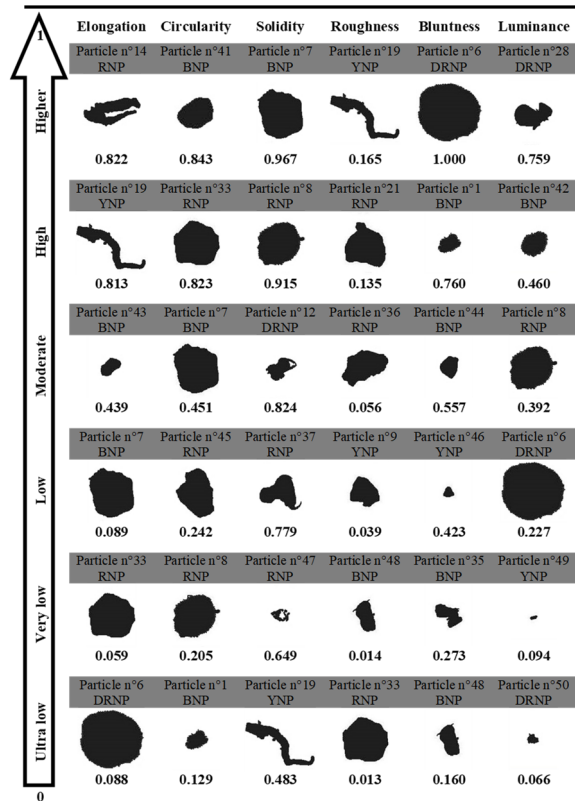


Figure 5: General classification of particles according their shape parameters.

The ultra-low value to express solidity of these particles is 0.483 and indicates that these particles have globally a good solidity.

## 4 CONCLUSIONS

This study showed that the size estimation of particulate material is a complicated matter. The results highlight the fact that particle size distributions may not be unique. Different techniques can give a large range of different parameters which need to be interpreted correctly. The choice of the parameters also depends on the purpose of the research. It is shown that particle shape analysis that includes the full range of available grain sizes can contribute not only measurements of particle size and shape, but also information on size-dependent densities and specific surface area. Based on these results obtained after an experimental testing program and an important data analysis, the following conclusions can be drawn for the volcanic scoria powders that have been tested here:

In addition to the PSD ; particle shape and surface morphology of ground materials can be quantitatively determined using the IA.

The particle size and the shape of these powders can be quantitatively determined by using the IA supported by digital analysis methods.

A methodology can be established to study the particle size and shape distribution of SCMs.

Shape parameters provide quantitative, meaningful and reproducible measurements of particle morphology if chosen carefully.

A discrepancy was observed between the IA and the LD size distributions toward both the lower and upper sizes.

The grain size data of the volcanic scoria powders are strongly dependent on shape parameters of particles, and shape heterogeneity was different between different size classes.

This description is absolutely needed for understanding particles' behavior in contact with water when used in cementitious materials.

## ACKNOWLEDGEMENTS

The first author would like to thank Mrs. Sophie Leroy and Mr. Frédéric Michel, GeMMe research engineers at the University of Liège (Belgium) for their help in the testing program.

## REFERENCES

- Abazarpoor, A., Halali, M., Hejazi, R., Saghaeian, M., 2017. *HPGR effect on the particle size and shape of iron ore pellet feed using response surface methodology*, Mineral Processing and Extractive Metallurgy, pp. 1-9.
- Arvaniti, E. C., Juenger, M. C. G., Bernal, S. A., Duchesne, J., Courard, L., Leroy, S., Provis, J. L., Klemm, A., De Belie, N., 2015a. *Physical characterization methods for supplementary cementitious materials*, Materials and Structures, 48(11):3675–3686.
- Arvaniti, E. C., Juenger, M. C. G., Bernal, S. A., Duchesne, J., Courard, L., Leroy, S., Provis, J. L., Klemm, A., De Belie, N., 2015b. *Determination of particle size, surface area, and shape of supplementary cementitious materials by different techniques*, Materials and Structures, 48(11):3687–3701.
- Bagheri, G. H., Bonadonna, C., Manzella, I., Vonlanthen, P., 2015. *On the characterization of size and shape of irregular particles*, Powder Technology, 270:141–153.
- Bouglada, M. S., Naceri, A., Baheddi, M., Pereira-de-Oliveira, L., 2019. *Characterization and modelling of the rheological behaviour of blended cements based on mineral additions*, European Journal of Environmental and Civil Engineering, pp. 1-18.
- Bouyahyaoui, A., Cherradi, T., Abidi, M. L., Tchamdjou, W. H. J., 2018. *Characterization of particle shape and surface properties of powders from volcanic scoria*, Journal of Materials and Environmental Science, 9(7):2032-2041.
- Califice, A., Michel, F., Dislaire, G., Pirard, E., 2013. *Influence of particle shape on size distribution measurements by 3D and 2D image analyses and laser diffraction*, Powder Technology, 237:67–75.
- Dioguardi, F., Mele, D., Dellino, P., 2018. *A new one-equation model of fluid drag for irregularly shaped particles valid over a wide range of Reynolds number*, J. of Geophysical Res.:Solid Earth, 123:144–156.
- EN 196-6., 2010. *Methods of testing cement - Part 6: Determination of fineness*, European Standard.
- Felekoglu, B., 2009. *A new approach to the characterisation of particle shape and surface properties of powders employed in concrete industry*, Construction and Building Materials, 23:1154–1162.
- Ferraris, C. F., Hackley, V. A., Aviles, A. I., Buchanan, C. E., 2002. *Analysis of the ASTM round-Robin test on particle size distribution of Portland cement: Phase I*, Report no. 6883. Maryland: National Institute of Standards and Technology (NISTIR).
- Gregoire, M. P., Dislaire, G., Pirard, E., 2007. *Accuracy of size distributions obtained from single particle static digital image analysis*, Proceeding. PARTEC Conference. Nuremberg, 4p.
- Hackley, V. A., Lum, L-S., Gintautas V., Ferraris, C. F., 2004. *Particle size analysis by laser diffraction spectrometry: application to cementitious powders*, Report no. 7097. Maryland: National Institute of Standards and Technology (NISTIR).

- He, H., Courard, L., Pirard, E., Michel, F., 2016. *Shape analysis of fine aggregates used for concrete*, Image Anal Stereol, 35:159-166.
- Ilic, M., Budak, I., Vucinic, M., Nagode, A., Kozmidis-Luburic, U., Hodolic, J., Puskar, T., 2015. *Size and shape particle analysis by applying image analysis and laser diffraction-inhalable dust in a dental laboratory*, Measurement, 66:109–117.
- Jia, X., Garboczi, E. J., 2016. *Advances in shape measurement in the digital world*, Particuology, 26:19–31.
- Juimo, W. H. T., Grigoletto, S., Michel, F., Courard, L., Cherradi, T., Abidi, M. L., 2017. *Effects of various amounts of natural pozzolans from volcanic scoria on performance of Portland cement mortars*, International Journal of Engineering Research in Africa, 32:36-52.
- Juimo, W., Cherradi, T., Abidi, L., Oliveira, L., 2016. *Characterisation of natural pozzolan of "Djoungo" (Cameroon) as lightweight aggregate for lightweight concrete*, GEOMATE, 11(27):2782-2789. <https://doi.org/10.21660/2016.27.1310>.
- Klemm, A. J., Wiggins, D. E., 2017. *Particle size characterisation of SCMs by mercury intrusion porosimetry*, Fizyka Budowli W Teorii I Praktyce Tom IX, Nr 1-2017, pp 5-12.
- Liu, E. J., Cashman, K. V., Rust, A. C., 2015. *Optimising shape analysis to quantify volcanic ash morphology*, GeoResJ, 8:14–30.
- Michel, F., Courard, L., 2014. *Particle size distribution of limestone fillers: granulometry and specific surface area investigations*, Particulate Science and Technology, 32:334-340.
- Mikli, V., Käerdi, H., Kulu, P., Besterci, M., 2001. *Characterization of powder particle morphology*, Proceedings of the Estonian Academy of Sciences, Engineering 7(1):22–34.
- Niesel, K., 1973. *Determination of the specific surface by measurement of permeability*, Materials and Structures, 6(3):227-231.
- Orhan, M., Özer, M., Işık, N., 2004. *Investigation of laser diffraction and sedimentation methods which are used for determination of grain size distribution of fine grained soils*, G.U. Journal of Science, 17(2):105–113.
- Pavlović, M. G., Pavlović, L. J., Maksimović, V. M., Nikolić, N. D., Popov, K. I., 2010. *Characterization and morphology of copper powder particles as a function of different electrolytic regimes*, International Journal of Electrochemical Science, 5:1862–187.
- Tchamdjou, W. H. J., Cherradi, T., Abidi, M. L., De Oliveira, L. A. P., 2017a. *Influence of different amounts of natural pozzolan from volcanic scoria on the rheological properties of Portland cement pastes*, Energy Procedia, 139:696–702. DOI: 10.1016/j.egypro.2017.11.274.
- Tchamdjou, W. H. J., Abidi, M. L., Cherradi, T., De Oliveira, L. A. P., 2017b. *Effect of the color of natural pozzolan from volcanic scoria on the rheological properties of Portland cement pastes*, Energy Procedia, 139:703–709. DOI: 10.1016/j.egypro.2017.11.275.
- Tierrie, J., Baaj, H., Darmedru, P., 2016. *Modeling the relationship between the shape and flowing characteristics of processed sands*, Construction and Building Materials, 104:235–246.
- Varga, G., Kovács, J., Szalai, Z., Cserhádi, C., Újvári, G., 2018. *Granulometric characterization of paleosols in loess series by automated static image analysis*, Sedimentary Geology, 370, pp 1-14.